Inclusion of Pre-Existing Undervoltage Load Shedding Schemes in AC-QSS Cascading Failure Models

Sina Gharebaghi, *Student Member, IEEE,* Sai Gopal Vennelaganti, *Student Member, IEEE,* Nilanjan Ray Chaudhuri, *Senior Member, IEEE,* Ting He, *Senior Member, IEEE,* and Thomas La Porta, *Fellow, IEEE*

Abstract—A challenging problem facing AC-Quasi-Steady-State (AC-QSS) cascading failure models of power system is the divergence issue primarily stemming from voltage collapse phenomena. In reality, there are undervoltage load shedding (UVLS) relays, which aim to prevent such a collapse by shedding a pre-specified fraction of load at buses where the corresponding voltages fall below a threshold. However, capturing the UVLS action in QSS models is very difficult, because most of the time the model cannot generate an equilibrium below the voltage threshold due to divergence. To address this problem, current models have applied different variants of uniform load shedding (ULS) till convergence is achieved, which differ from the ground truth. In order to solve this, we propose a methodology that leverages the post-ULS load flow as a starting point when divergence occurs. In this condition, a sensitivity index coupled with the voltage magnitudes of buses is used to recognize the buses that are most prone to voltage collapse. The UVLS scheme is then applied to these buses. To verify the accuracy of the results, we also present a suitable dynamic cascade model with appropriate limits and protection details that can selectively capture UVLS action, thereby revealing the proximate ground truth. Predictions of the proposed model are validated against those of the dynamic model for representative cases in IEEE 118-bus system. In addition, results of the proposed model are contrasted with two ULS schemes on the $2,383$-bus Polish system.

Index Terms—AC-QSS model, Cascading failure, Dynamic model, Under Voltage Load Shedding, UVLS, Voltage collapse.

I. Introduction

UNDERVOLTAGE load shedding (UVLS) schemes play an important role in saving the power grid from potential voltage collapse during cascading failures. The UVLS relays in a network typically shed a fixed fraction of noncritical loads at buses where voltages have gone below a certain threshold [1] for a pre-determined time. The most comprehensive UVLS architectures involving local protection relays and centralized remedial action schemes (RASs) are present in the US Western Electricity Coordinating Council (WECC) system [2]–[4]. Models that do not consider such existing schemes end up showing highly pessimistic results in terms of total demand served at the end of cascade – an important measure of the

severity of such events. In this context, we remark that AC-Quasi-Steady-State (QSS) model [5]–[13], [27], [28] is the only computationally manageable model that can capture the voltage stability issues. However, incorporating existing UVLS schemes in the AC-QSS cascading failure models remains an open problem.

In absence of a UVLS scheme the AC-QSS model often diverges during cascade propagation, which can be primarily attributed to voltage instability. How often such divergence will occur depends on the system characteristics. To the best of our knowledge, current AC-QSS models [5]–[13], [27], [28] cannot include pre-existing UVLS schemes that shed loads only at those buses that go below a threshold. When divergence is observed during cascade, such models typically consider uniform load shedding (ULS) i.e., each bus sheds the same pre-defined fraction of load irrespective of its voltage magnitude [6], [9], [11], [12]. A stochastic cascade model is proposed in [13] in which the divergence issue is addressed via continuation power flow (CPF) [14]. However, authors have not mentioned the potential problems regarding the choice of initial point for CPF. Moreover, when Q-limits are considered, depending on the initial point, CPF may lead to completely different $P-V$ curves due to $PV-PQ$ bus switching. Reference [10] applies DC optimal power flow (OPF) for load shedding when AC-QSS model diverges. Authors in [12] introduce a model based on AC OPF considering frequency deviations to simulate the remedial control when system collapse happens.

Typical AC-QSS models [5]–[13] fail to capture the voltage threshold-based UVLS relays in practical systems [1]–[4] since most of the time the models cannot generate an equilibrium below the voltage threshold due to divergence. Therefore, such models may result in a cascade path that is completely different from the ground truth.

The other challenge is to find a way to validate the results of any proposed model that considers an existing UVLS scheme. Dynamic cascading failure models like [15]–[17], [22]–[26] can be used to generate the ground truth corresponding to the post-UVLS equilibrium. Unlike QSS-type models, dynamic models are capable of representing realistic UVLS schemes as they output temporal evolution of voltages, and therefore do not encounter the problem of divergence unless the UVLS scheme fails to arrest the collapse. The problem however is that they also reflect dynamic phenomena involving angle stability and other nonlinearities that might arise due to controller limit hitting, and so on. Therefore, one needs to be thoughtful

in introducing certain modifications in the dynamic model and consider scenarios that avoid these interactions before validating the AC-QSS results.

The contribution of this paper is twofold – first, we propose a methodology to represent the UVLS scheme in an AC-QSS model that builds on our preliminary work [32], and second, we present a suitable dynamic cascade model with appropriate limits and protection details that can selectively capture UVLS action, thereby revealing the proximate ground truth. To that end, the post-ULS load flow [6], [9], [11], [12] is used as a starting point when divergence occurs. In this condition, a sensitivity index coupled with the voltage magnitudes of buses are used to recognize the buses that are most prone to voltage collapse. The UVLS scheme is then applied to these buses. In order to impose Q limits in the dynamic model consistent with the AC-QSS model, we propose a new field voltage limiting scheme as a function of the machine current injection. We validate results of the proposed AC-QSS model against a few representative cases in the dynamic model of the IEEE 118-bus test system. Finally, statistical analysis is performed to compare the results of cascading failures obtained from the proposed AC-QSS model and the traditional AC-QSS model equipped with two ULS-type schemes for a large-scale $2,383$-bus Polish network.

II. AC-QSS Model: Challenges in Including Pre-Existing UVLS Schemes

We first look into AC-QSS cascading failure models in literature and how they deal with the divergence issue. Next, we elaborate on the challenge facing inclusion of local voltage threshold-based UVLS relays in AC-QSS models.

A. State-of-the-art AC-QSS Cascading Failure Models

In this section, we provide an overview of AC-QSS models proposed in [6], [9], [10], [12], [27] – a detailed benchmarking analysis was done in [28]. The cascading failure are triggered with a set of initial failures. Various islands might form due to the initial outages. The load and the generation are first balanced in each island by tripping excess generation/load, and the cascade model is applied individually on each island, thereby mimicking underfrequency relay action. In each tier of cascade, the cascade propagates by tripping overloaded branches using overcurrent relays. These trippings will change the topology of each island and might result in new island formation. Once the load flow diverges in an island, i.e. voltage collapse is observed, the models proposed different variants of uniform load shedding (ULS) until convergence is achieved. If no convergence is obtained, a blackout is assumed to happen in the island. The cascade is stopped when either no overloaded line is observed or no more load is available to be served in the island due to a complete blackout. For the sake of comparison, a simple ULS-based AC-QSS model including the above-mentioned steps is used as a first benchmark in this paper.

As an intelligent variant of ULS, we also consider the commonly-known Manchester model proposed in [6], [27], where the authors assume that the system operators have

enough time to react to divergence of the power flow (PF). This does not represent local autonomous UVLS relay action – rather operator intervention-based action. Nevertheless, we introduce an AC-QSS model as a second benchmark with a smarter shedding strategy similar to the Manchester model. In this model called 'Manchester-type model', if PF diverges in an island, we divide the island into different subgraphs/areas and we start load shedding in the subgraphs starting with the highest absolute mismatch between active generation and load until convergence is achieved. The mismatch is weighted by the real power load in the subgraph normalized by the total load in the island. To the best of our knowledge, [6], [27] do not provide any specific definition of an 'area'. Therefore, we have formed an algorithm to create such areas as will be described in Section V.

B. UVLS Schemes and Challenges of Including them in AC-QSS Models

The UVLS relays in a network typically shed a fixed fraction of loads at buses where voltages have gone below a certain threshold and remain there for a predetermined period of time – typically $3 − 5$ s [1]–[4]. There are two types of UVLS schemes: decentralized and centralized. The decentralized scheme relies upon local relay actions at individual load centers whereas the centralized schemes involve high speed communication of sensor data to control center and more complex rule-based tripping mechanisms – such schemes are called RASs or special protection schemes. *The focus of this paper is on the decentralized UVLS schemes.*

WECC guidelines [4] indicate that UVLS is designed based on coordination between protection and planning engineers to avoid tripping under faults and heavy loading conditions that do not lead to voltage collapse. The schemes act when voltage collapse is likely to occur – this is where AC-QSS models face major issues since they represent "snapshot" of steady state conditions. Therefore, the condition of voltage collapse leads to divergence of load flow in the first place and the UVLS shedding cannot be applied. Moreover, the idea of applying CPF [14] to solve this issue is quite challenging since it was not tailored for cascading failure application – more specifically, we have observed that depending on the initial point on the $P − V$ curve and the $PV − PQ$ bus switching, one might end up in completely different trajectories.

Clearly, the current AC-QSS models [5]–[13] do not have the means to include decentralized UVLS schemes, which lead to a different cascade propagation path.

III. Proposed Method

In this section, we propose an improved AC-QSS model enabled by new indices, which is capable of modeling decentralized UVLS schemes. This is one of the key contributions of the paper. The proposed AC-QSS model has been implemented using MATPOWER [21]. Figure 1 depicts the flowchart of the proposed model, which consists of three layers – L_{body}, L_{conv}, and L_{div}. The body-layer (L_{body}) contains the traditional AC-QSS model that includes overcurrent tripping, island formation, and load balancing. The other layers (L_{conv}

and L_{div}) deal with converged and diverged PFs in an island for closely mimicking the behavior of UVLS relays. Variables v_i indicates the voltage magnitude of bus i and v_{th} indicates a pre-specified voltage magnitude below which the UVLS relay is programmed to trip a fraction $(1-r)$ of the pre-disturbance load. Also, let k_{shed}^i and k_{shed}^{max} be integers denoting the number of UVLS trippings at bus i and the maximum allowable number of trippings at each bus, respectively. Note that v_{th}, r, and k_{shed}^{max} are pre-designed parameters of the UVLS scheme used as input to our model – we are not proposing any new design methodology in our paper. The UVLS action at bus i would be in the following form:

$$D_{load}^i = r^{k_{shed}^i}(D_{load}^{i,pre}),$$
$$k_{shed}^i \in [0, 1, ..., k_{shed}^{max}] \tag{1}$$

where, $D_{load}^{i,pre}$ indicates the pre-disturbance load at node i, and D_{load}^i is load at bus i after load shedding is applied. We note that for constant impedance load, D refers to the load admittance, whereas it refers to real and reactive power for its constant power counterpart.

The proposed AC-QSS model starts in the L_{body} layer with a set of initial node outages. In the next step, the model forms the resulting islands (if any) due to initial node outages. Upon formation, let $P_{mm} = P_{load} + P_{loss} - P_{gen} > 0$ in an island, where P_{load}, P_{loss}, and P_{gen} are the total real power load, loss, and generation, respectively in that island. In reality, that island goes through governor action (R_G being governor droop coefficient) to increase generation and in parallel may undergo underfrequency load shedding (UFLS), if frequency falls below a threshold – Fig. 2 shows a typical primary frequency response. To emulate this in the AC-QSS model, we apply an iterative approach as shown in Fig. 2 that leads to the post-disturbance equilibrium.

First, we assume that there is no UFLS action. So, mismatch will solely be addressed by increasing active generation (P_G) of generators through governor action. In steady state we have (with typical notations):

$$\Delta P_{G,i} = -\frac{\Delta f}{R_{G,i}}, \Delta f = -\frac{P_{mm}}{\sum_{i=1} \frac{1}{R_{G,i}}}, f_1 = f_0 + \Delta f,$$
$$P_{G,i} = P_{G,i_0} + \Delta P_{G,i} \tag{2}$$

As shown in Fig. 2, the value of f_1 is updated iteratively and if f_1 is less than a threshold f_{th} (59.5 Hz in this paper) plus a tolerance ϵ (assumed 0.1 Hz), UFLS action takes place.

If $P_{mm} < 0$, there will be a surplus of active power generation. In this case, power mismatch will solely be compensated by governor action by decreasing P_G of generators.

For each island, PF is conducted – if convergence is achieved, we move to the L_{conv} layer. If $v_i \leq v_{th}$ for at least one bus, we proceed to find the 'candidate buses' for load tripping as described in Section III-A.

On the other hand, if PF diverges in the island, the L_{div} layer will be applied. First, the diverged network is saved as Net_{div}^{int}. To identify the candidate buses for load shedding we need a converged PF case. To that end, in an intermediate step, we apply ULS on Net_{div}^{int} that trips a uniform fraction of loads in all buses until convergence is achieved. Then,

we calculate our proposed Candidate Bus Identification (CBI) index (described next), on the converged solution to identify candidate buses for load shedding.

Finally, we apply UVLS in candidate buses in the pre-ULS diverged network (Net_{div}^{int}) iteratively till convergence is achieved. The process of checking bus voltages below threshold and load shedding is repeated till all voltages come above threshold or k_{shed}^{max} is reached. If no convergence is achieved in the intermediate ULS stage or after k_{shed}^{max} is reached in the candidate buses during UVLS, the island is assumed to have a complete blackout.

A. Indices to Identify the Candidate Buses

We propose a two-step approach to determine the candidate buses that are more likely to undergo UVLS. To that end, we either directly use the converged solution of PF in an island, or for the diverged PF case, obtain a converged PF using ULS (if it exists). In the first step, we calculate a weakness index of buses in this condition based upon $V - Q$ sensitivity. Next, we combine this information with the voltage magnitude of buses to propose a composite CBI index.

1) Weakness index: For the converged cases, the process described in this section to calculate weakness index uses the converged PF. For the diverged cases, we argue that the PF solution with ULS brings us close to the voltage collapse point, which allows us to evaluate the bus voltages that are most sensitive to loading. We hypothesize that these are the buses whose voltages are more likely to dip below v_{th} and undergo load shedding. We use the Jacobian matrix to calculate the most sensitive buses in the network [18]. The linearized relationship between incremental change in bus active and reactive power with incremental change in bus voltage angle and magnitude is as follows:

$$\begin{bmatrix} \Delta P \\ \Delta Q \end{bmatrix} = \begin{bmatrix} J_{P\theta} & J_{Pv} \\ J_{Q\theta} & J_{Qv} \end{bmatrix} \begin{bmatrix} \Delta \theta \\ \Delta v \end{bmatrix} \tag{3}$$

In [18] authors proposed the sensitivity index, also called weakness index in this paper, for buses based on $Q - V$ sensitivity, so $\Delta P = 0$ is assumed. Using (3), ΔQ can be written as follows:

$$\Delta Q = [J_{Qv} - J_{Q\theta}J_{P\theta}^{-1}J_{Pv}]\Delta v = J_R \Delta v \tag{4}$$

and,

$$\Delta v = J_R^{-1} \Delta Q \tag{5}$$

where, the J_R indicates the reduced Jacobian matrix of the system:

$$J_R = [J_{Qv} - J_{Q\theta}J_{P\theta}^{-1}J_{Pv}] \tag{6}$$

By decomposition approach, J_R can be written as:

$$J_R = \xi \Lambda \eta \tag{7}$$

where ξ, η, and Λ present the right eigenvector matrix, left eigenvector matrix, and diagonal eigenvalue matrix of J_R, and,

$$J_R^{-1} = \xi \Lambda^{-1} \eta \tag{8}$$

or,

$$\Delta v = \sum_k \frac{\xi_k \eta_k}{\lambda_k} \Delta Q \tag{9}$$
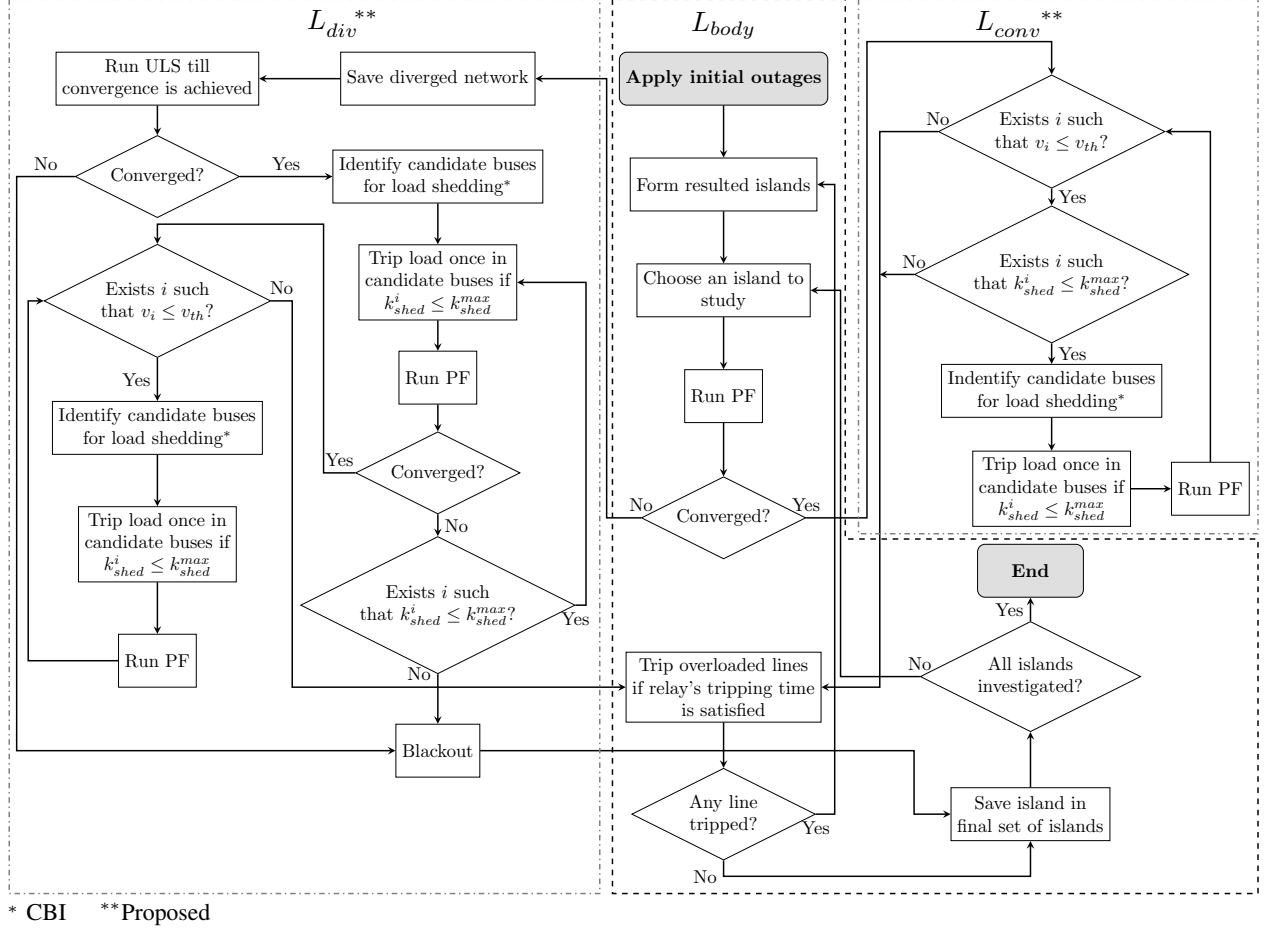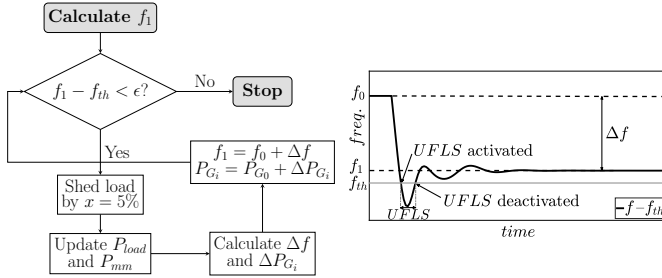
Fig. 1: Flowchart of the proposed model.

Fig. 2: Left: Iterative process of implementing governor action and UFLS in AC-QSS model. Right: Typical primary frequency response.

where, ξ_k and η_k show the right and left eigenvector of J_R, respectively, and k indicates the mode number. We can reformulate (9) as follows:

$$\Delta v_i = \sum_k \frac{\xi_{ki}\eta_{ik}}{\lambda_k} \Delta Q_i, \quad \forall i \qquad (10)$$

with ξ_{ki} and η_{ik} the ith element of ξ_k and η_k, where i indicates i^{th} bus. So, we can formulate the $V-Q$ sensitivity of bus i as:

$$\frac{\partial v_i}{\partial Q_i} = \sum_k \frac{\xi_{ki}\eta_{ik}}{\lambda_k} = \sum_k \frac{\mathcal{P}_{ik}}{\lambda_k}, \quad \forall i \qquad (11)$$

where,

$$\mathcal{P}_{ik} = \xi_{ki}\eta_{ik} \qquad (12)$$

$\mathcal{P}_{ik}$ is defined as participation factor/weakness index of bus i to mode k. It indicates the contribution of kth eigenvalue, pertinent to mode k, to the $V-Q$ sensitivity at bus i.

The smaller eigenvalues are associated with the weak modes of the system. So we can use m smallest eigenvalues to identify the weakest buses in the system [18], [19]. A higher value of $\mathcal{P}_{ik}$ for bus i shows higher sensitivity for bus i in mode k.

Remark: The weakness index calculation involves inversion of Jacobian submatrix $J_{p\theta}$, which is sparse and inversion of reduced Jacobian J_R, which is dense. Matlab [29] typically uses LU factorization in this process, which is based on a variant of Gaussian elimination. When inverting the $n \times n$ dense matrix J_R, the order of complexity in such algorithms, e.g. recursive block LU algorithm is typically $\mathcal{O}(n^3)$ [33]. For the sparse matrix inversion, the complexity typically depends upon the number of nonzero entries, rather than the matrix dimension.

2) CBI index: At the converged solution (either obtained directly from the converged PF or with ULS), the buses can be categorized as (Fig. 3) –

1. Voltage: Low, Weaknesses index: High;

2. Voltage: Low, Weakness index: Low;
3. Voltage: High, Weakness index: High;
4. Voltage: High, Weakness index: Low.

Clearly, buses in the last category have the lowest chance to qualify as candidate buses, whereas the first has the highest, and the remaining have moderate chances. Based upon these logical arguments, we propose the CBI index as:

$$CBI_i = \frac{v_{th}-v_i}{\max_i |v_{th}-v_i|} + \frac{\mathcal{P}_i}{\max_i(\mathcal{P}_i)} \qquad (13)$$

where, $\mathcal{P}_i$ denotes the weakness index $\mathcal{P}_{ik}$ in which the k is the mode with smallest eigenvalue. As can be seen in (13), the proposed index for bus i is the sum of the voltage deviation from v_{th} and it's weakness index – each normalized with respect to their maximum values.

Next, we sort the buses according to a descending order of the CBI index. Now, it is time to finalize the list of candidate buses for load shedding. To do so, we identify the last bus f with $v_f - v_{th} - \gamma \leq 0$ from the list of the ordered buses, where γ is a user-defined parameter indicating conservatism in our selection, i.e. higher the value of γ the lesser the chance of misses. We select buses 1 to f as our final candidate buses for load shedding.
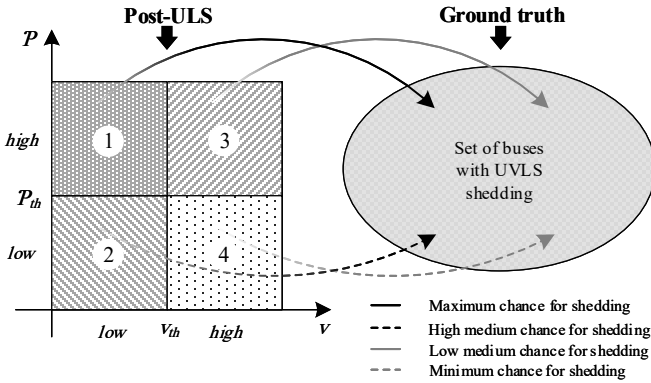

Fig. 3: Basis for proposing CBI index: Qualitative mapping of chance of candidate buses to the ground truth set that have undergone UVLS shedding.

Remarks: (1) In the flowchart in Fig. 1, the 'Run PF' block takes into account governor action and UFLS (when appropriate), and distributes loss among generators in proportion to their inverse governor droops during power flow.
(2) The impact of operation of UVLS on other protection schemes can be quite complex depending on the operating condition and the system configurations. For example, UVLS schemes will reduce load consumption, which may lead to reduction in line current that affect overcurrent protection, and arrest frequency nadir, thereby impacting UFLS action.

IV. DYNAMIC MODEL FOR VALIDATING AC-QSS MODEL WITH UVLS SCHEME

In the existing literature, a few papers including [15]–[17], [22]–[26] discussed the details of the suitable model required to perform cascading failure studies. These works focused on different aspects of cascading simulation, like models suitable for parallel computing [22], probabilistic risk assessment [23], hybrid modeling and corrective action under extreme weather [24], modeling protection relay behavior during cascade [25], and optimal investment to improve grid resilience and restoration following cascading failure [26]. Reference [15] built upon traditional dynamic models used to study transient stability and added multiple protection functionalities to perform cascading failure study. However, in the context of UVLS, one of the main differences between the AC-QSS model and the traditional dynamic models arises because of the fact that the former uses explicit reactive power limits Q_{max} and Q_{min} on generators, whereas the latter employ field heating limits (FHL) instead of reactive power limits. Since the reactive power capability of generators plays a major role during analysis of UVLS phenomena, this aspect needs significant attention. In this paper, we present a suitable dynamic model with appropriate limits and protection details to selectively capture UVLS action, as described next.

A. Dynamic Model Selectively Capturing UVLS Action

The proposed dynamic model has been developed using the basic building blocks in Matlab/Simulink [29] from first principles. In this model, a standard static constant impedance, current, power, and exponential ($ZIPE$) load representation, along with phasor modeling of transmission network is considered. To represent the generators, a sixth-order subtransient model equipped with excitation systems and governors with appropriate time constants is chosen. Both IEEE DC1A and IEEE ST1A exciters were separately taken into account. Details about the generator, exciter, and governor models can be found in [20], and are not repeated here. However, magnetic saturation and armature resistance were ignored in this model. Also, a different $d-q$ reference frame consistent with IEEE standard modeling is considered where the d axis leads the q axis.

Two main features were included in this dynamic model, (i) protection relays and (ii) limits. The former includes line overload tripping, over and underfrequency generator tripping, UFLS, and UVLS – each with their corresponding time delay units. As part of the second category, real power limits are enforced by directly limiting the mechanical torque input to the generator. However, in order to enable a comparative study between the dynamic and the AC-QSS model, the excitation limits are modified in a way such that the constant minimum and maximum reactive power limits of the AC-QSS model can be replicated.

Figure 4(a) shows how the capability curve of Generator #5 in IEEE 118 bus system's dynamic model, specifically the overexcitation and underexcitation limits are different from the constant maximum and minimum reactive power limits of that generator in AC-QSS model, respectively. Assuming 1 pu voltage at the terminal, for various armature currents at maximum and minimum reactive power, the limits of the excitation voltage E_{fd} are calculated using generator model during the steady state conditions. Figure 4(b) shows how the AC-QSS constant reactive power limits are reflected in the field voltage and armature current plane, when compared to
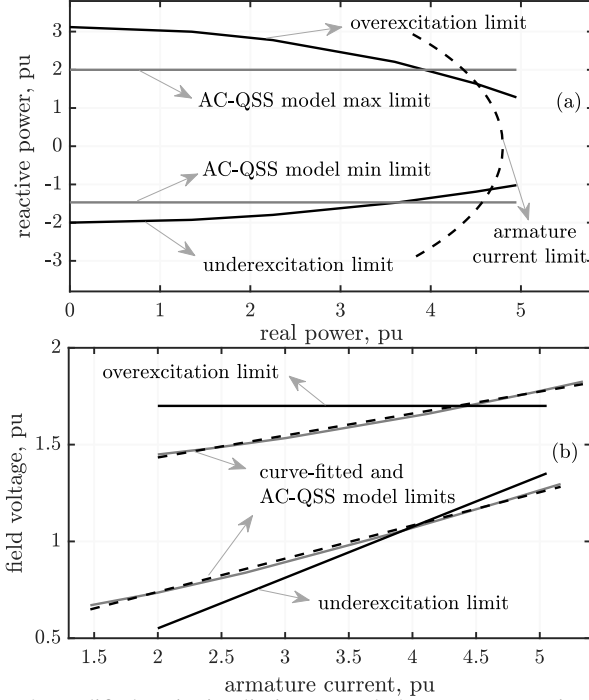
Fig. 4: Modified excitation limits to match the constant reactive power limits of the AC-QSS model for a fair comparative study.

actual over and underexcitation limits. The AC-QSS model based limits are linearly curve fitted as shown in 4(b) and those lines are used as excitation limit in the dynamic model to match the reactive characteristics of AC-QSS model.

Apart from the proposed approach to enforce explicit reactive power limits, the salient features of the dynamic model are as follows: (a) *Load model* – Although the model is generic, i.e. it can handle any mixture of components in the $ZIPE$ load, we have simulated 100% constant Z and 100% restorative constant P loads. In the first case, the Y_{bus} subsumes the load admittance with zero current injection from load buses. In the constant P load case, we have introduced a delay reflecting the restorative characteristics [30] – the model is shown in Fig. 5. Here, P_0 and Q_0 are the nominal real and reactive power loads, and $P_t(V) = |V|^\alpha$, $Q_t(V) = |V|^\beta$.
(b) *UVLS model* – The UVLS relays apply a block-averaging algorithm to measure the mean voltage in a moving window that spans over duration same as the time delay of UVLS. If the mean voltage goes below the threshold in a window filled with samples, load shedding happens. Following each shedding, the minimum time before the next allowed shedding is set at the predefined delay.
(c) *UFLS model* – If the center of inertia (COI) frequency falls and stays below 59.5 Hz for at least 1 s, then UFLS action takes place.
(d) *Load shedding implementation* – For a constant Z case, the Y_{bus} is changed in a discrete manner during load shedding. For the other load type, value of $P_0 + jQ_0$ is changed in Fig. 5 in a step-like manner that results in a smooth change in current injection.
(e) *Solver* – We use solvers $ode23tb$ for constant Z case and $ode23$ (Bogacki-Shampine) for restorative load case. These are proven off-the-shelf variable-step solvers from Mat-

lab/Simulink [29].

B. Validation of the Proposed AC-QSS Model

We validate the proposed AC-QSS model by comparing results from the first tier of cascade with our proposed dynamic model in the IEEE 118-bus network shown in Fig. 6. The reason behind not going beyond the first tier is that the system becomes more stressed and severe nonlinearities will impact the response of the dynamic model, which can not be used to validate the accuracy of the AC-QSS model. Both the models are equipped with pre-designed UVLS relays with the following parameters: $v_{th} = 0.91 \times 0.95 = 0.8645$ pu, $k_{shed}^{max} = 5$, and $r = 0.75$. For the AC-QSS model with UVLS scheme γ is assumed to be equal to 0.0 pu. For the dynamic model, the UVLS scheme trip loads if voltage at the corresponding buses stay below v_{th} continuously for 5 s. For the sake of fair comparison of AC-QSS model with the dynamic one, we intentionally prevent the dynamic model to trip overloaded lines during the simulation period.

Constant Impedance Load: First, 100% constant Z load is considered in the dynamic model. For AC-QSS model, we convert the nominal loads into equivalent admittances and include them in the Y_{bus}. We consider three representative cases with $8\%, 9\%$, and 10% initial node outage (based on the fact that they have higher fraction of initial nodal outage and that all of them lead to divergence of PF in the largest island) for comparison.

1) Time-domain response from dynamic models: First, we present simulation results to demonstrate the effectiveness of the proposed dynamic model in the context of its suitability for representing Q limits in AC-QSS model. Figure 7 shows the variation in reactive power output of four synchronous generators following 8% initial node outage at $t = 5$ s. It can be seen that the proposed model respects the Q-limits of the AC-QSS model under steady state, whereas the traditional (FHL) model does not.

Figures 8 – 10 show the voltage variation in selected buses following initial node outages at $t = 5$ s and subsequent UVLS-based load trippings in the proposed dynamic model. We consider these results to be the proximate ground truth. The load tripping instances can be identified through jumps in the voltage profile – trippings as low as two times in Case 3 and as high as five times in Case 2 can be observed. Note that the trippings are not necessarily taking place at the buses themselves, since such trippings elsewhere will also introduce transients in each bus voltage.
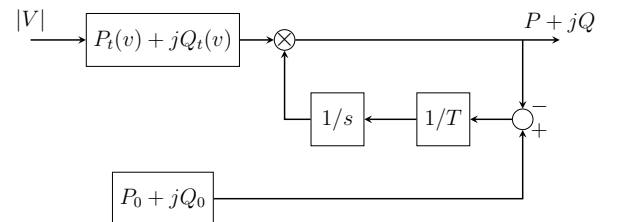

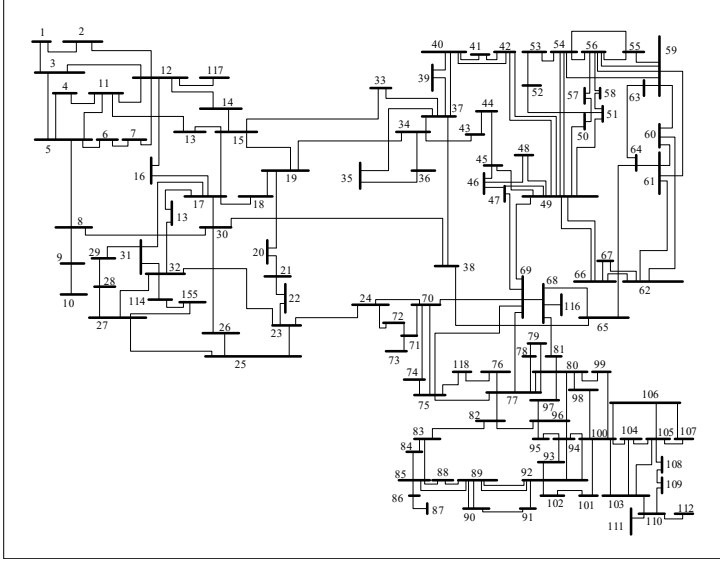Fig. 5: Restorative constant power load model.
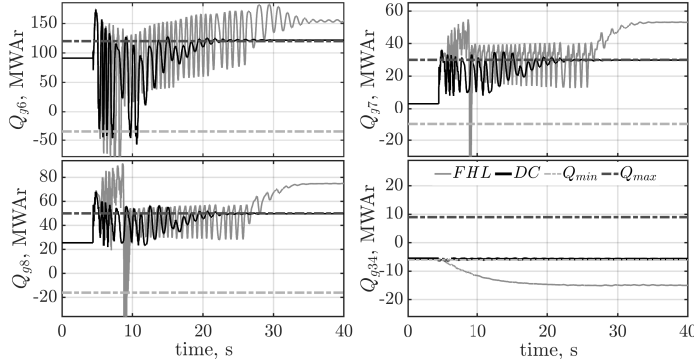
Fig. 6: One-line diagram of IEEE 118-bus system.

Fig. 7: Case 1: Reactive power generation of selected generators following 8% initial node outage at $t = 5$ s in traditional (FHL) and proposed dynamic models (DC) – both with DC1A exciters.

All the previous cases considered a IEEE DC1A exciter model. To see the effect of a static excitation system, we simulated the cases with IEEE ST1A model – the voltage variations for Case 1 is shown in Fig. 11. A comparison with Fig. 8 show that the responses have minor differences in transient behavior. Similar observations were made for other cases, which are not reported here due to space constraints.

2) Comparison of UVLS results: Table I provides bus location and number of load trippings in the following models: (1) traditional dynamic model with DC1A exciter (k^{FHL}), (2) proposed dynamic model with DC1A exciter (k^{DC}), (3) proposed dynamic model with ST1A exciter (k^{ST}), and (4) proposed AC-QSS model (k^{AC}). Table II summarizes the number of misses and false trippings in the proposed AC-QSS model with respect to different dynamic models. Table III presents comparison of misses and false trippings of AC-QSS model with UVLS when compared against 25 more dynamic simulation cases with DC1A exciter for initial node outages varying between $5-10\%$. In each case, the number of misses and false alarms are calculated as a percentage of total number of trippings in the dynamic model. The following is the summary of observations:
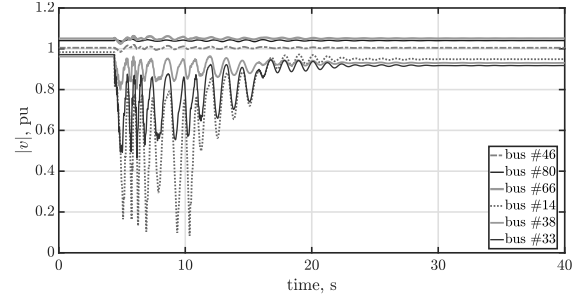

Fig. 8: Case 1: Voltage variation in selected buses following 8% initial node outage at $t = 5$ s and subsequent load tripping due to UVLS relays: IEEE DC1A model for exciter.
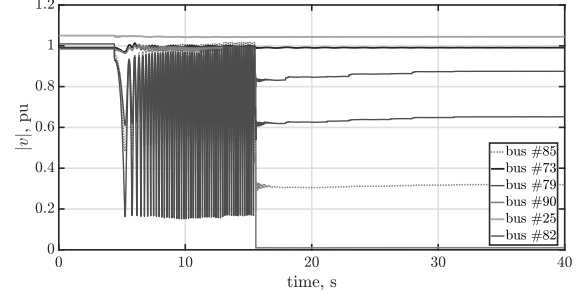

Fig. 9: Case 2: Voltage variation in selected buses following 9% initial node outage at $t = 5$ s and subsequent load tripping due to UVLS relays: IEEE DC1A model for exciter.

Fig. 10: Case 3: Voltage variation in selected buses following 10% initial node outage at $t = 5$ s and subsequent load tripping due to UVLS relays: IEEE DC1A model for exciter.
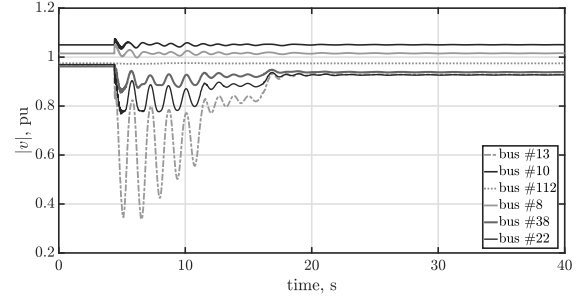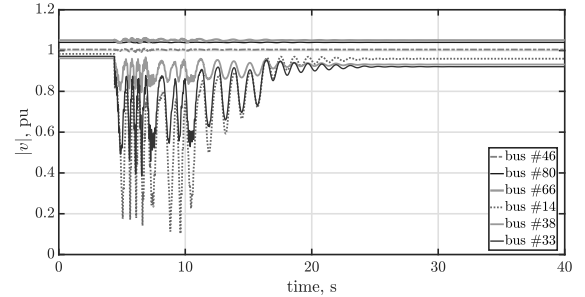

Fig. 11: Case 1: Voltage variation in selected buses following 8% initial node outage at $t = 5$ s and subsequent load tripping due to UVLS relays: IEEE ST1A model for exciter.

- Table I indicates that the proposed dynamic models equipped with IEEE DC1A and ST1A exciters produce near identical results in terms of the location and number of UVLS sheddings, whereas the traditional dynamic model with FHL produces a different outcome. As also

TABLE I: Location and Number of Load Trippings in Dynamic and AC-QSS Models: IEEE 118-Bus System

#	case 1					case 2					case 3				
	bus	k^{DC}	k^{ST}	k^{FHL}	k^{QSS}	bus	k^{DC}	k^{ST}	k^{FHL}	k^{QSS}	bus	k^{DC}	k^{ST}	k^{FHL}	k^{QSS}
1	1	2	2	5	2	77	4	4	2	5	1	2	2	3	2
2	2	2	2	5	2	78	4	4	2	5	2	2	2	3	2
3	3	2	2	5	2	79	4	4	2	5	3	2	2	3	2
4	6	2	2	5	1	82	5	5	5	5	6	1	1	2	1
5	7	2	2	5	1	83	5	5	5	5	7	1	1	2	1
6	11	2	2	5	2	84	5	5	5	5	11	2	2	3	2
7	12	2	2	5	1	85	5	5	5	5	12	2	1	3	1
8	13	2	2	5	2						13	2	2	3	2
9	14	2	2	5	2						14	2	2	3	2
10	15	2	2	5	2						15	2	2	3	2
11	16	2	2	5	2						16	2	2	3	2
12	18	2	2	5	2						18	2	2	2	2
13	19	2	2	5	2						19	2	2	2	2
14	20	2	2	5	2						20	2	2	2	2
15	33	2	2	5	2						21	2	2	2	2
16	34	0	0	2	0						22	1	1	1	0
17	117	2	2	5	2						33	2	2	2	2
18											117	2	2	3	2

TABLE II: Number of Misses and False Trippings in Proposed AC-QSS Model w.r.t. Different Dynamic Models: IEEE 118-Bus System

		Ground truth		
		DC1A	ST1A	FHL
case 1	miss	3	3	53
	fauls trip	0	0	0
case 2	miss	0	0	0
	fauls trip	3	3	9
case 3	miss	2	1	14
	fauls trip	0	0	0

TABLE III: Number of Misses and False Trippings in 25 Separate Cases with IEEE DC1A Exciter: IEEE 118-bus System

	mean	min	max
miss, %	7.368262	0	25
false trippings, %	2.930844	0	18.18182

TABLE IV: Location and Number of Load Trippings in Dynamic Model with Restorative Load and AC-QSS Model: IEEE 118-Bus System

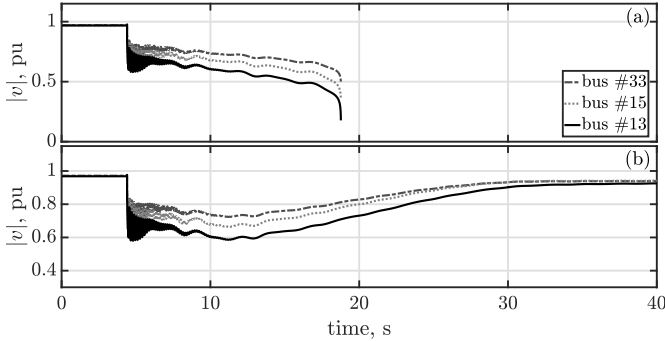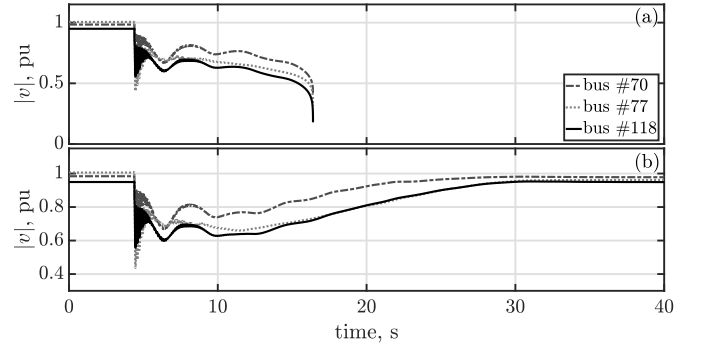| #	case 4			case 5			case 6		
	bus	k^{DC}	k^{QSS}	bus	k^{DC}	k^{QSS}	bus	k^{DC}	k^{QSS}
1	13	4	3	70	2	1	76	2	2
2	14	2	2	74	3	1	77	3	2
3	15	3	3	75	3	2	78	3	2
4	18	3	2	76	4	2	79	3	2
5	19	3	3	77	3	2	82	4	2
6	20	3	3	78	3	2	83	4	2
7	21	3	3	79	3	2	84	4	2
8	22	3	2	82	3	1	95	4	3
9	33	3	2	83	2	1	96	4	3
10	34	2	2	84	0	1	97	4	3
11	35	2	2	95	1	1	118	1	2
12	36	2	2	96	2	1			
13	37	0	2	97	2	1			
14	43	2	2	118	3	2			
15	44	0	1						

Fig. 12: Case 4: Voltage variation in selected buses following 7% initial node outage at $t = 5$ s and subsequent load tripping due to UVLS relays: IEEE DC1A exciter and restorative load model.

Fig. 13: Case 5: Voltage variation in selected buses following 5% initial node outage at $t = 5$ s and subsequent load tripping due to UVLS relays: IEEE DC1A exciter and restorative load model.

indicated by Table II, traditional FHL models are not suitable for benchmarking the AC-QSS model's UVLS performance.

- Based on Tables I and II, when benchmarked w.r.t. the proposed dynamic model, almost all the bus locations that had undergone UVLS-based trippings have been correctly identified by the AC-QSS model, except load at bus 22 in Case 3 not being captured by the AC-QSS model. Only 3 false alarms are observed for Case 2.
- As observed from Tables I and II, the number of trippings have some differences between the proposed AC-QSS and the proposed dynamic models – nevertheless, they

are reasonably close to each other. Table III shows that, although in certain cases there can be as high as 25% misses and 18% false trippings, the average total error (misses plus false trippings) is around 10%.

Restorative Constant Power Load: Next, 100% constant P load with restorative characteristics is considered in the dynamic model, while the AC-QSS model assumes constant power loads. For the restorative model $\alpha = 0.6$, $\beta = 3.0$, $T = 3.0$ s are assumed, and UVLS tripping delay of 5 s is considered as before. Each case considers DC1A excitation system in our proposed model. We take into account three separate cases with 7% initial node outages in two (Cases 4
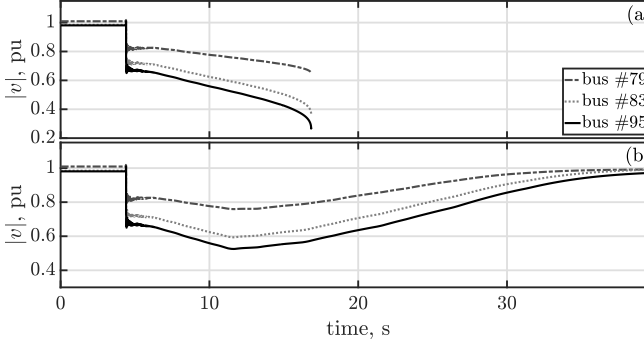
Fig. 14: Case 6: Voltage variation in selected buses following 7 initial node outage at $t = 5$ s and subsequent load tripping due to UVLS relays: IEEE DC1A exciter and restorative load model.

and 6) and 5% outage in one (Case 5) – the largest island in AC-QSS model without UVLS diverges in each case.

3) Time-domain response from dynamic models: Figures 12, 13, and 14 show the time-domain response following initial node outages at $t = 5$ s. In absence of UVLS relays, the system witnesses voltage collapse as indicated by Fig. 12(a), 13(a), and 14(a). On the other hand, the presence of the decentralized UVLS scheme saves the system from voltage collapse as shown in 12(b), 13(b), and 14(b).

4) Comparison of UVLS results: Table IV shows the comparison of bus location and number of sheddings due to UVLS relays between the AC-QSS and the dynamic model. It can be observed that we obtain reasonably close match between these results, given that all buses undergoing UVLS has been captured by the AC-QSS model.

These extensive studies give us confidence in the proposed model and allow us to perform exhaustive Monte-Carlo simulations with the AC-QSS models based on ULS, Manchester-type, and UVLS schemes.

V. CASE STUDIES

The IEEE 118-bus system and the Polish network during winter $1999 - 2000$ peak condition [21] are studied here to contrast UVLS, ULS, and Manchester-type AC-QSS models. To create subgraphs/areas in the Manchester-type model, we first order the generators/loads in each island according to the degree of the corresponding bus. Then we build subgraphs around them consecutively, considering a predetermined number h of hops (4 for 118-bus and 30 for Polish system) from the root node. We ignore the nodes that are already included by an existing subgraph. This procedure is repeated until we cover all the nodes. In this context, we use words 'subgraph' and 'area' interchangeably.

For the IEEE 118-bus system, different initial node outages varying from $1\% - 9\%$ of total nodes are tested. Afterwards, cases with initial node outages varying from $1\% - 5\%$ are studied for the Polish system. For each case, 500 Monte Carlo runs were performed with random selection of node outages. When faced with divergence, the ULS scheme iteratively sheds load in the fraction of 0.5% uniformly in all load buses till convergence is achieved – no load is shed if we have a converged PF. The shedding strategy in Manchester-type model was discussed in Section II-A. For UVLS, the same
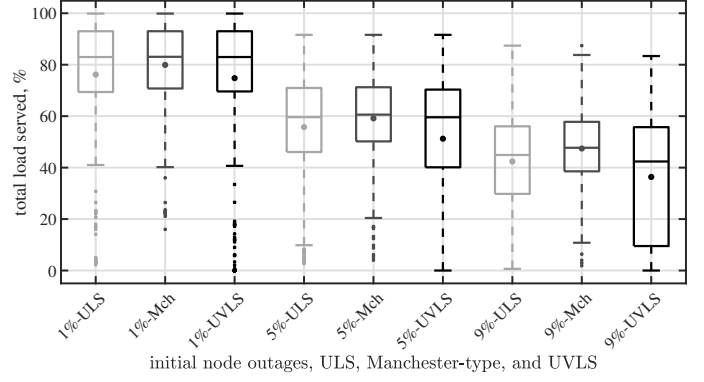

Fig. 15: Boxplots of total load served at the end of cascade comparing ULS, Manchester-type, and UVLS in IEEE 118-bus system: 500 Monte Carlo runs were conducted for each % of initial nodal outage.
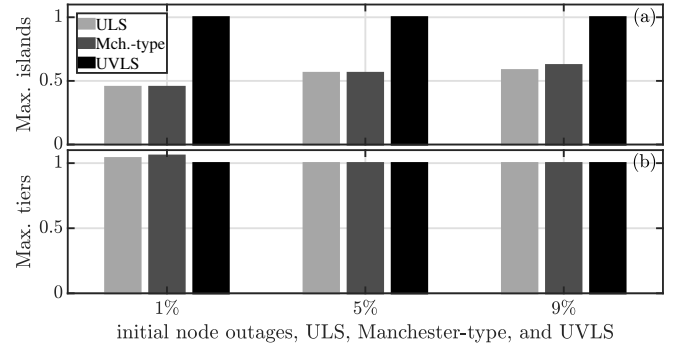

Fig. 16: Cascade outcome comparison for ULS, Manchester-type, and UVLS: IEEE 118-Bus System.

settings that were mentioned earlier are applied. For the IEEE 118-bus cases, $\gamma = 0.02$ pu and for the Polish network, $\gamma = 0.05$ pu is assumed. A constant impedance load model is considered in the studies.

In addition, we have performed probabilistic analysis using two metrics: distribution of number of lines out and demand loss [28]. Probability of outage of each bus is assumed to be $5e - 4$, based on [31]. The metrics help compare paths for cascade propagation in ULS, Manchester-type model, and UVLS.

A. IEEE 118-bus System

Figure 15 represents the box-whisker plots of total demand served the end of cascade, which compares ULS, Machester-type, and UVLS models. The line inside each box represents the median, the bottom and the top edges of the box cover data in the first ($Q1$) and the third ($Q3$) quartile, respectively; whereas the corresponding whiskers indicate $Q1 - 1.5(Q3 - Q1)$ and $Q3 + 1.5(Q3 - Q1)$. The outliers are excluded from whiskers, which are plotted using small dots. Finally, the mean values are marked using big dots. It can be observed that the mean value is slightly higher in the ULS model compared to the proposed model – the median value, however is almost the same. Moreover, the inter-quartile range is higher for UVLS. For Manchester-type model, the mean value is the highest and the inter-quartile range is the tightest among others. It is expected, since the Manchester-type model represents more intelligent shedding that presumes operator intervention as

opposed to autonomous local shedding in a decentralized UVLS scheme.

Figure 16 shows some additional variables comparing the outcome of the cascading process, namely number of maximum islands and tiers normalized with respect to UVLS cases. The following is the summary of observations:

- On a consistent basis, the normalized maximum number of islands formed out of 500 runs is much higher for UVLS cases.
- The maximum number of tiers are relatively close to each other.

The distribution of number of lines out and total demand served at the end of cascade are shown in Figs 17 and 18, respectively. In this analysis, we assume that the initial node outages are independent events. These are indicators of cascade propagation paths in different models under consideration. Figure 17 indicates that from 30% or higher demand loss, the cascade propagation paths of these models start diverging – Manchester-type model gives highly optimistic results followed by ULS. On the other hand, this effect can be observed beyond approximately 75 line outages (Fig. 18), albeit with less pronounced difference between Manchester-type and ULS models.

B. Polish System

Figure 19 shows the comparison of maximum number of islands formed and maximum number of tiers of cascade
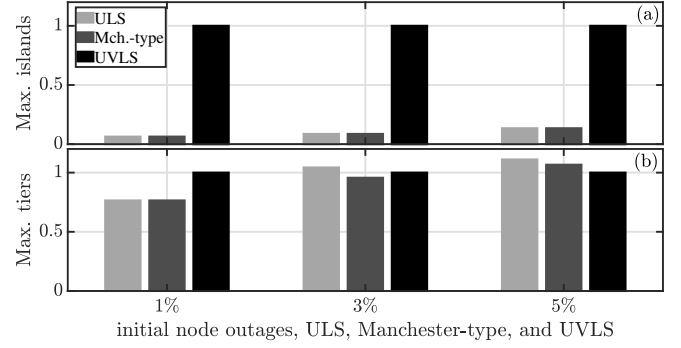

Fig. 19: Cascade outcome comparison for ULS, Manchester-type, and UVLS: Polish System

across different initial outages for ULS, Manchester-type, and UVLS models. These metrics are normalized with respect to the UVLS model. It can be seen that UVLS leads to many more islands compared to the other models, whereas the maximum number of tiers of cascade are relatively similar across the three models.

We have also compared the cascade propagation paths of the three models considering distribution of demand loss and distribution of line outages through probabilistic analysis [28]. As before, we assume that the initial node outages are independent events. This leads to a significantly low probability even for 1% node outage in the Polish system (assuming probability of each node outage as $5e-4$). We plot the distribution of
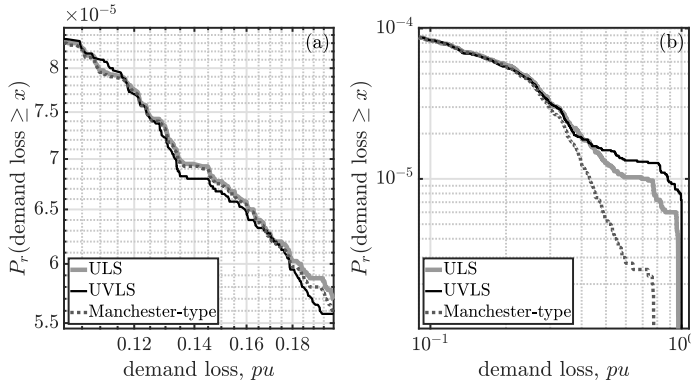

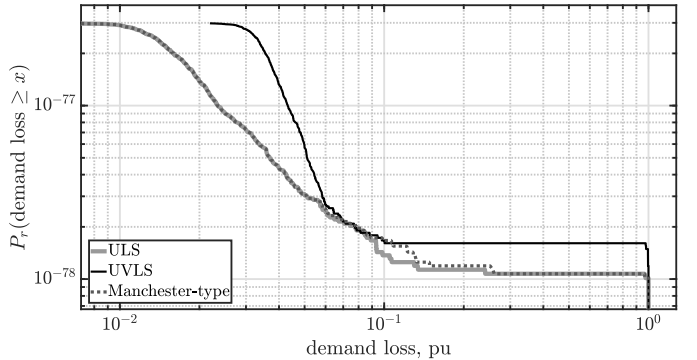Fig. 17: Distribution of demand loss: IEEE 118-bus system.

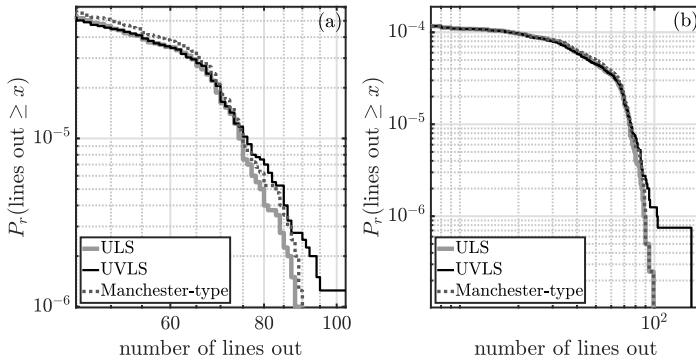Fig. 20: Distribution of demand loss: Polish system.

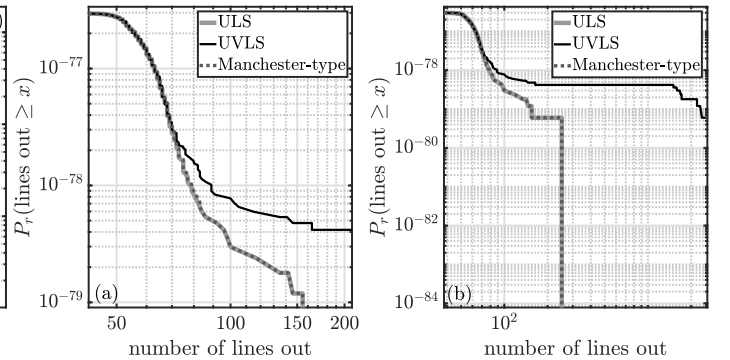Fig. 18: Distribution of line outage: IEEE 118-bus system.

Fig. 21: Distribution of line outage: Polish system.

demand loss in Fig. 20. This plot reveals that UVLS leads to higher demand loss corresponding to the same cumulative probability when compared with ULS and Manchester-type shedding. Interestingly, the ULS and UVLS cases lead to almost same distribution.

We have also compared the cumulative probability of line outage for these three models. As shown in Fig. 21, the propagation paths for ULS and Manchester-type model are very similar. The propagation path of UVLS starts departing beyond ≈ 70 or more line outages.

C. Average CPU Time for Cascade Simulation

The approximate average runtime for entire cascade process of 1 Monte Carlo run for ULS and UVLS models are 2 s and 3 s for IEEE 118-bus network, and 21 s and 36 s for the Polish system, respectively. In the proposed model, the process of calculating CBI-index $(3) - (12)$ is taking approximately 0.03 s for IEEE 118-bus network, and 1.6 s for Polish system on average. We ran these simulations in MATLAB on an AMD Ryzen 7 3800X CPU with 32 GB RAM.

VI. CONCLUSION

This paper proposed a new methodology for inclusion of pre-existing UVLS relays in the AC-QSS model for cascading failure and a new field voltage limiting approach in dynamic model for validating its accuracy. A reasonably close match was obtained between the results of these two models in IEEE 118-bus system at the end of first tier of cascade. Extensive Monte Carlo simulations on IEEE 118-bus system and $2,383$-bus Polish system indicate that in contrast with UVLS, the ULS approach used in literature leads to a significantly different path of cascade propagation resulting in an optimistic estimate of total demand served at the end of cascade. The proposed models can be used to improve offline planning study of cascading failure for a given UVLS scheme in the system.
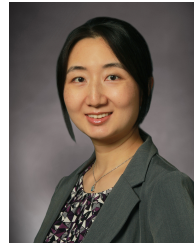
ACKNOWLEDGMENT

REFERENCES

[1] C. J. Mozina, "Undervoltage load shedding," 2007 60th Annual Conference for Protective Relay Engineers, College Station, TX, pp. 16-34, 2007.

[2] North American Electric Reliability, Council guidelines for developing an under voltage load shedding (UVLS) evaluation program, Sep. 2006.

[3] R. Verayiah, A. Mohamed, H. Shareef, and I. Z. Abidin. "Review of under-voltage load shedding schemes in power system operation," 2014.

[4] Western Systems Coordinating Council, undervoltage load shedding guidelines, Jul. 1999.

[5] D. Bienstock, "Adaptive online control of cascading blackouts," 2011 IEEE Power and Energy Society General Meeting, Detroit, MI, USA, pp. 1-8, 2011.

[6] D. P. Nedic, I. Dobson, D. S. Kirschen, B. A. Carreras, and V. E. Lynch, "Criticality in a cascading failure blackout model," International Journal of Electrical Power & Energy Systems, vol. 28, i. 9, pp. 627-633, 2006.

[7] M. Almassalkhi and I. Hiskens, "Model-predictive cascade mitigation in electric power systems with storage and renewables, Part I: Theory and implementation," 2015 IEEE Power & Energy Society General Meeting, Denver, CO, pp. 1-1, 2015.

[8] M. R. Almassalkhi and I. A. Hiskens, "Model-predictive cascade mitigation in electric power systems with storage and renewables—part II: Case-study," IEEE Trans. Power Syst., vol. 30, no. 1, pp. 78-87, Jan. 2015.

[9] S. Mei, Y. Ni, G. Wang and S. Wu, "A study of self-organized criticality of power system under cascading failures based on AC-OPF with voltage stability margin," IEEE Trans. Power Syst., vol. 23, no. 4, pp. 1719-1726, Nov. 2008.

[10] Q. Chen and L. Mili, "Composite power system vulnerability evaluation to cascading failures using importance sampling and antithetic variates," IEEE Trans. Power Syst., vol. 28, no. 3, pp. 2321-2330, Aug. 2013.

[11] J. Li, C. Shi, C. Chen, L. Dueñas-Osorio, "A cascading failure model based on AC optimal power flow: Case study," Physica A: Statistical Mechanics and its Applications, vol. 508, pp. 313-323, 2018.

[12] W. Ju, K. Sun and R. Yao, "Simulation of cascading outages using a power-flow model considering frequency," IEEE Access, vol. 6, pp. 37784-37795, 2018.

[13] M. H. Athari and Z. Wang, "Stochastic cascading failure model with uncertain generation using unscented transform," IEEE Trans. Sust. Energy.

[14] V. Ajjarapu and C. Christy, "The continuation power flow: a tool for steady state voltage stability analysis," IEEE Trans. power systems, vol. 7, no. 1, pp. 416-423, Feb. 1992.

[15] J. Song, E. Cotilla-Sanchez, G. Ghanavati and P. D. H. Hines, "Dynamic modeling of cascading failure in power systems," IEEE Trans. Power Syst., vol. 31, no. 3, pp. 2085-2095, May 2016.

[16] S. K. Khaitan, Chuan Fu and J. McCalley, "Fast parallelized algorithms for on-line extended-term dynamic cascading analysis," 2009 IEEE/PES Power Systems Conference and Exposition, Seattle, WA, pp. 1-7, 2009.

[17] X. Gao, M. Peng, C. K. Tse and H. Zhang, "A Stochastic Model of Cascading Failure Dynamics in Cyber-Physical Power Systems," in IEEE Systems Journal.

[18] B. Gao, G. K. Morison and P. Kundur, "Voltage stability evaluation using modal analysis," in IEEE Transactions on Power Systems, vol. 7, no. 4, pp. 1529-1542, Nov. 1992.

[19] William J. Stewart, and Allan Jennings. "A simultaneous iteration algorithm for real matrices", ACM Transaction on Mathematical Software, Vol. 7. No. 2. pp. 184-198, June 1981.

[20] Sauer, P.W. and Pai, M.A, "Power System Dynamics and Stability," Prentice Hall, 1998.

[21] R. D. Zimmerman, C. E. Murillo-Sanchez. MATPOWER User's Manual, Version 7.0. 2019.

[22] C. Parmer, E. Cotilla-Sanchez, H. K. Thornquist, and P. D.H. Hines, "Developing a dynamic model of cascading failure for high performance computing using trilinos," in Proceedings of the first international workshop on High performance computing, networking and analytics for the power grid (HiPCNA-PG '11), Association for Computing Machinery, pp. 25–34.

[23] P. Henneaux, P. Labeau, J. Maun, and L. Haarla, "A Two-Level Probabilistic Risk Assessment of Cascading Outages," in IEEE Transactions on Power Systems, vol. 31, no. 3, pp. 2393-2403, May 2016.

[24] M. R. Vallem et-al., "Hybrid cascading outage analysis of extreme events with optimized corrective actions," 2017 19th International Conference on Intelligent System Application to Power Systems (ISAP), San Antonio, TX, 2017, pp. 1-6.

[25] A. J. Flueck, I. Dobson, Z. Huang, N. E. Wu, R. Yao, and G. Zweigle, "Dynamics and Protection in Cascading Outages," 2020 IEEE Power & Energy Society General Meeting (PESGM), Montreal, QC, 2020, pp. 1-5.

[26] B. J. Pierre, B. Arguello, and M. J. Garcia, "Optimal Investments to Improve Grid Resilience Considering Initial Transient Response and Long-term Restoration," 2020 International Conference on Probabilistic Methods Applied to Power Systems (PMAPS), Liege, Belgium, 2020, pp. 1-6.

[27] B. M. Rios, K. Bell, D. Kirschen, and R. Allan, "Computation of the Value of Security: Final Project Report Volume I," available online https://labs.ece.uw.edu/real/Library/Reports/Value of Security Part I.pdf.

[28] P. Henneaux et al., "Benchmarking Quasi-Steady State Cascading Outage Analysis Methodologies," 2018 IEEE International Conference on Probabilistic Methods Applied to Power Systems (PMAPS), Boise, ID, 2018, pp. 1-6.

[29] MATLAB. (2020). 9.9.0.1524771 (R2020b). Natick, Massachusetts: The MathWorks Inc.

[30] W. Xu and Y. Mansour, "Voltage stability analysis using generic dynamic load models," IEEE Trans. Power Syst., vol. 9, no. 1, pp. 479-493, Feb. 1994.

[31] R. Billinton and R. N. Allan, "Reliability Evaluation of Power Systems," 2nd ed. New York: Plenum, 1996.

[32] S. Gharebaghi, S. G. Vennelaganti, N. R. Chaudhuri, T. He and T. L. Porta, "Solving the divergence problem in AC-QSS cascading failure model by introducing the effect of a realistic UVLS scheme," 2020 IEEE PES Innovative Smart Grid Technologies Europe (ISGT-Europe), The Hague, Netherlands, 2020, pp. 710-714.

[33] G. H. Golub, and C. F. Van Loan, "Matrix Computations," Fourth ed. JHU Press, 2013.

Ting He (SM'13) is an Associate Professor in the School of Electrical Engineering and Computer Science at Pennsylvania State University, University Park, PA. Her work is in the broad areas of computer networking, network modeling and optimization, and statistical inference. Dr. He is a senior member of IEEE, an Associate Editor for IEEE Transactions on Communications (2017-2020) and IEEE/ACM Transactions on Networking (2017-2021), and an Area TPC Chair of IEEE INFOCOM (2021). She received multiple Outstanding Contributor Awards from IBM, and multiple paper awards from ITA, ICDCS, SIGMETRICS, and ICASSP.

Sina Gharebaghi (S'17, S'20) received the B.Sc. degree in Electrical Engineering from Urmia University, Urmia, Iran, in 2016, and the M.Sc. degree in Electrical Engineering from the Sharif University of Technology, Tehran, Iran, in 2018. He is currently a graduate research assistant and Ph.D. student in the School of Electrical Engineering and Computer Science at The Pennsylvania State University, University Park, PA. His research interests include power system dynamics and stability, cascading failures, and power flow analysis.

Sai Gopal Vennelaganti (S'16-M'21) received his bachelor's degree in electrical engineering from the Indian Institute of Technology Madras, India, in 2016, and Ph.D. degree from Pennsylvania State University, USA, in 2020. He is currently an Engineer/Scientist with the Grid Operations and Planning Research and Development group, EPRI, Knoxville, TN, USA. His research interests include modeling and prevention of cascading failure in cyber-physical power systems, topology estimation, power system stability, and control applications in HVDC, multi-terminal HVDC, power quality, hybrid microgrids and smart grids.

Thomas F. La Porta (F'02) is the Director of the School of Electrical Engineering and Computer Science and Penn State University. He is an Evan Pugh Professor and the William E. Leonhard Chair Professor in the Computer Science and Engineering Department and the Electrical Engineering Department. He received his B.S.E.E. and M.S.E.E. degrees from The Cooper Union, New York, NY, and his Ph.D. degree in Electrical Engineering from Columbia University, New York, NY. He joined Penn State in 2002. He was the founding Director of the Institute of Networking and Security Research at Penn State. Prior to joining Penn State, Dr. La Porta was with Bell Laboratories for 17 years. He was the Director of the Mobile Networking Research Department in Bell Laboratories, Lucent Technologies where he led various projects in wireless and mobile networking. He is an IEEE Fellow, Bell Labs Fellow, received the Bell Labs Distinguished Technical Staff Award, and an Eta Kappa Nu Outstanding Young Electrical Engineer Award. He also won two Thomas Alva Edison Patent Awards. His research interests include mobility management, signaling and control for wireless networks, security for wireless systems, mobile data systems, and protocol design. Dr. La Porta was the founding Editor-in-Chief of the IEEE Transactions on Mobile Computing. He served as Editor-in-Chief of IEEE Personal Communications Magazine. He has published numerous papers and holds 39 patents.

Nilanjan Ray Chaudhuri (S'08-M'09-SM'16) received the Ph.D. degree in power systems from Imperial College London, London, UK in 2011. From 2005 to 2007, he worked in General Electric (GE) John F. Welch Technology Center. He came back to GE and worked in GE Global Research Center, NY, USA as a Lead Engineer during 2011 to 2014. Presently, he is an Associate Professor with the School of Electrical Engineering and Computer Science at Penn State, University Park, PA. He was an Assistant Professor with North Dakota State University, Fargo, ND, USA during 2014-2016. He is a member of the IEEE and IEEE PES. Dr. Ray Chaudhuri is the lead author of the book Multi-terminal Direct Current Grids: Modeling, Analysis, and Control (Wiley/IEEE Press, 2014). He served as an Associate Editor of the IEEE TRANSACTIONS ON POWER DELIVERY (2013 – 2019) and IEEE PES LETTERS (2016 - present). Dr. Ray Chaudhuri was the recipient of the National Science Foundation Early Faculty CAREER Award in 2016 and Joel and Ruth Spira Excellence in Teaching Award in 2019.